JOURNAL OF GEOPHYSICAL RESEARCH, VOL. 106, NO. D2, PAGES 1655–1667, JANUARY 27, 2001

"Synoptic" estimates of chemically active species and other diurnally varying parameters in the stratosphere, derived from measurements from the Upper Atmosphere Research Satellite (UARS)

Frank T. Huang

Science Systems and Applications Inc., Lanham, Maryland

Carl A. Reber

NASA Goddard Space Flight Center, Greenbelt, Maryland

Abstract. Over the past two decades there have been numerous articles in the literature discussing methods of obtaining global-scale "synoptic" mathematical representations from asynoptic satellite observations. These studies cover a wide range of viewpoints, ranging from claims of presenting synoptic maps to opinions stating that synoptic representations cannot be obtained from asynoptic data alone, and that physical models are needed to augment the measurements. We review and comment on many of these previous studies. We do not believe that previous published representations generated from Upper Atmosphere Research Satellite data alone for variables that exhibit significant diurnal variations, are indeed synoptic. However, we show that UARS data can be used to estimate useful synoptic approximations without the need for physical models. Using a two-dimensional Fourier least squares algorithm, we calculate mathematical approximations to "synoptic maps." We provide examples for ClO, $ClONO_2$, NO_2, O_3, CH_4, temperature, and winds and discuss how they can provide new information on both the chemistry and dynamics of the atmosphere.

1. Introduction

Satellites that sound the Earth's stratosphere have made available an enormous amount of information with near-global coverage. Obviously however, a given satellite cannot make measurements simultaneously over a large portion of the globe, so single-satellite observations are always asynoptic. As used here, synoptic measurements refer to data taken simultaneously over a wide spatial area [*Huschke*, 1970]. Parameters which have significant diurnal variations should be represented with their local solar times varying in a consistent manner with the corresponding longitudes, for a particular date and Greenwich mean time (GMT).

Over the past two decades or so, there have been numerous papers in the literature presenting methods (with very different conclusions) for generation of "synoptic" maps from asynoptic measurements. Several papers claim that the maps they present are synoptic, while others state that synoptic representations cannot be obtained from asynoptic data alone and that physical models are needed to augment the measurements. We believe that calling any of these representations "synoptic" is inaccurate in the strict sense of the word and that they all provide approximations in varying degrees to what one would obtain if true synoptic data were available, including both longitudinal and local time effects. It appears that most of the published approaches have their own sets of advantages and shortcomings, some emphasizing longitudinal-type effects, including traveling waves, while others emphasize diurnal or other types of effects.

In the following, we use data from the Upper Atmosphere Research Satellite (UARS) [*Reber*, 1993; *Reber et al.*, 1993] to expand on a mapping algorithm presented previously [*Huang et al.*, 1997] and discuss its relationship to other approaches for representing atmospheric data. Previous articles in the literature related to synoptic maps include those by *Rodgers* [1976], *Salby* [1982], *Haggard et al.* [1986], *Lait and Sanford* [1988], *Elson and Froidevaux* [1993], *Sassi and Salby* [1998], and *Khattatov et al.*, [1999]. With the exception of *Khattatov et al.* these approaches use either the Fourier transform technique by *Salby* [1982] or the sequential estimation technique of *Rodgers* [1976]. They all claim that the maps which they present are synoptic. On the other hand, *Khattatov et al.* state that the *Salby* [1982] method does not generate truly synoptic maps. They also discuss the UARS level 3B (L3B) data, based (with variants) on the sequential algorithm described by *Rodgers* [1976] (see section 2.3), and assert that the L3B data are not synoptic. *Khattatov et al.* [1999, p. 18,715] say that "It is shown that these methods are unable to produce truly synoptic maps of short-lived photochemically active species due to insufficient temporal and spatial density of satellite observations. The only way to overcome this limitation is to supplement observations with prior independent information given, for instance, by atmospheric numerical models and/or climatologies. Objective approaches to combining such prior information with observations are commonly referred to as data assimilation."

Paper number 2000JD900515.
0148-0227/01/2000JD900515$09.00

In agreement with *Khattatov et al.* [1999], we do not believe that the above-mentioned approximations produced either by the *Salby* [1982] method or by the sequential estimation technique are indeed synoptic; furthermore, the approximations are significantly poorer for variables that exhibit significant diurnal variations.

Unlike *Khattatov et al.*[1999], however, we believe that data from UARS afford the opportunity to approximate synoptic representations without the need for physical models. We present here what we believe are synoptic approximations derived from UARS L3B data, using the algorithm given by *Huang et al.*, [1997]. Although our examples focus on diurnal variations due primarily to chemical reactions and thermal tides, we also present estimates of local time effects related to longitude.

2. Review of Mathematical Representations of UARS Data

Because of the differing viewpoints, it seems appropriate to look in some detail at two methods which have been applied to UARS data, the Salby [1982] method and the sequential estimation technique (Rodgers, 1976; Haggard et al., 1986). It should be pointed out that the authors of the present paper are responsible for the UARS L3B data, generated using sequential estimation on a production basis by the UARS project. In the following, we discuss some of the issues that were addressed by *Khattatov et al.*[1999], but from a somewhat different perspective.

The method by *Salby* [1982] and the sequential estimation technique (as used with UARS data) are both Fourier series representations of the data. In addition to providing maps, mathematical representations can provide insight into physical processes such as identifying waves of particular frequencies. Our main interest here is how well these mathematical representations reflect the underlying physical processes. This depends on the following: (1) the information content of the data (e.g., the sampling pattern in space and time relative to the rate of changes in the atmosphere) and (2) mathematical considerations in being able to accurately retrieve and represent the information content of the data. To adequately characterize the physical processes, the data must have a sufficient sampling frequency in space-time, and the sampling grid pattern must be appropriate. It should be pointed out that these issues are relevant to both synoptic and asynoptic measurements.

Assume that measurements are made over a fixed latitude circle, at a given altitude, over 360° of longitude, and over a given time interval. We wish to estimate the Fourier coefficients

$$\{c_{nm}(z,\theta)\}$$

of the two-dimensional series

$$\Psi(t,z,\theta,\lambda)=\sum_n\sum_m c_{nm}(z,\theta)\, e^{i2\pi nt/T}\, e^{i2\pi m\lambda/2\pi} \quad (1)$$

from the data Ψ, where

z altitude;
λ longitude (radians);
θ colatitude;
t time;
n time wave number;
m longitudinal wave number;
T time interval of data selected.

For continuous data the Fourier coefficients can be obtained by the expression

$$c_{nm}(z,\theta) = \frac{1}{2\pi T}\int_0^T\int_0^{2\pi}\Psi(t,z,\theta,\lambda)\, e^{-i2\pi nt/T}\, e^{-i2\pi m\lambda/2\pi}\, d\lambda\, dt \quad (2)$$

due to the orthogonality properties of the of the trigonometric functions.

For the discrete case with a regular grid, orthogonality conditions also exist, and a numerical integration can take advantage of these conditions. If the sampling grid is irregular (e.g., an asynoptic satellite measurement grid, or simultaneous measurements on an irregular grid in space), the orthogonality conditions do not apply, and a numerical integration may yield biased estimates of the coefficients. Depending on the situation, it may be possible to overcome the irregular sampling and still obtain accurate estimates. However, if the data are undersampled in either space or time, the estimated coefficients may be aliased. Although we make the distinction between biases in the coefficients caused by irregular sampling and those caused by undersampling, the term "aliasing" is often used generally in situations where coefficients cannot be estimated uniquely.

2.1. Sampling Pattern and Information Content of UARS Data

The Upper Atmosphere Research Satellite (UARS) was launched by the Space Shuttle on September 12, 1991 into a near-circular orbit at 585 km altitude inclined 57° to the equator [*Reber et al.*, 1993]. These orbital parameters, combined with measurement characteristics for the limb-viewing atmospheric sensors, yield a measurement pattern that covers much of the globe on a daily basis. The instruments from which we use data here include the Cryogenic Limb Array Etalon Spectrometer (CLAES; *Roche et al.* [1993]), the Microwave Limb Sounder (MLS; *Waters* [1993]; *Barath et al.* [1993]), and the High Resolution Doppler Imager (HRDI; *Hays et al.* [1993]). CLAES and MLS view at 90° to the velocity vector, and can "see," over one orbit, to 80° latitude in one hemisphere and to 34° in the other. HRDI can view at other azimuths and normally sees to somewhat lower latitudes. This measurement pattern is further influenced by the precession of the orbit plane, which necessitates a yaw rotation of the spacecraft to maintain an orientation with one side pointed toward the Sun and the other side pointed away. This yaw of 180° occurs about every 36 days on average. Each yaw maneuver reverses the hemisphere with the highest latitude measurements, creating an approximate 36 day cycle that alternately favors the Northern or the Southern Hemisphere. The orbital period of 96.7 min leads to 14.9 orbits per day, or ~30 measurements per latitude per day.

Data are sampled at various latitudes because of the north/south motion of the satellite, and different longitudes

are sampled due to the rotation of the Earth relative to the orbital plane. Therefore it takes ~1 day to make measurements over the globe. The UARS sampling is such that for a given day, a given latitude, and a given orbital mode (heading north or heading south at the equator), the local solar times of the measurements are nearly constant (within 20 min) over all longitudes. Therefore, using both orbital modes, data are measured at essentially two distinct local solar times for a given day and latitude. However, since the orbital inclination is not 90°, these local times differ significantly for different latitudes. Because of orbital precession, the local solar times of the measurements decrease by ~20 min per day at each latitude, and it takes ~36 days to sample most of the full range of local time using data from both orbital modes. This sampling can be contrasted with that of Sun-synchronous satellites, where the local times of the measurements for a given orbital mode and latitude do not change from day to day. Additional details regarding UARS sampling are given by *Huang et al.* [1997].

This sampling pattern is such that for studies emphasizing local time effects, it is normally advantageous to divide the data by orbital mode so that local times are separated. For studies related to traveling waves or other geographically related phenomena, it is probably more advantageous to use measurements from both modes to double the amount of available data.

2.2. *Salby* [1982] Method

The method by *Salby* [1982] uses the mathematical representation in (1) and estimates the coefficients

$$\{c_{nm}(z,\theta)\}$$

from the data. It addresses the problem of asynoptic sampling and irregular grids in longitude, which can lead to biased estimates of the coefficients from the numerical integration of (2). Salby's method transforms the data so that longitudes do not overlap on successive days. Although this addresses the problem of irregular sampling, it does not correct all problems that can arise when aliasing is due to sampling at an inadequate rate. Because it takes a half day to sample all longitudes (using both orbital modes), the equivalent "Nyquist" frequency is one cycle per day, as pointed out by *Sassi and Salby* [1998]. Using this technique to generate maps of UARS temperature, O_3, H_2O, and N_2O, they state that the diurnal component is resolvable, but higher orders, such as the semidiurnal components, are not resolved. They claim that their maps are "synoptic". Although this may be true to an extent for variables that have relatively small diurnal variations, it appears that their approximation would not be particularly good for parameters that exhibit relatively large variations with local time, as semidiurnal components are generally not negligible in these cases.

Elson and Froidevaux [1993] furnish another example of the *Salby* [1982] technique. They state that synoptic maps can be constructed for any time during the observation period. However, the maps which they produce using both orbital modes combined are for temperature and O_3 and H_2O mixing ratios, all of which exhibit relatively small diurnal variations. For ClO mixing ratios, which have significantly more diurnal variation, they use ascending and descending mode data separately, while noting that their ClO maps do not show local time variation with longitude at a given latitude.

In both studies, maps were produced for parameters (e.g., temperature, O_3, and H_2O) that do not have significant diurnal variations on a percentage basis. In these cases, analysis and interpretation would be greatly facilitated if the diurnal variations were isolated and presented in that manner. We agree with *Khattatov et al.* [1999], in that the *Salby* [1982] method to date has not produced good synoptic approximations for diurnally varying parameters from UARS data alone. It should be noted that in both the above studies emphasis was on geographically related transport phenomena, which appear to be well characterized by Salby's technique.

2.3. Sequential Estimation

The *Salby* [1982] method retrieves a mathematical representation based on the data alone, without the benefit of physical models. One method that has the capability of using additional information (e.g., an equation of state, a priori data) is the sequential (recursive) method, based on the work of *Kalman* [1960]. Kalman filters have been used with success in satellite orbit/attitude determination and control [*Wertz,* 1986]). The sequential method provides for combining results from measured data with those from a priori information in a statistically optimal manner. *Rodgers* [1976] presented a variant of the Kalman filter, one that uses previous data (as opposed to a physical model) for a priori information. This is the basis for the mapped data from the Limb Infrared Monitor of the Stratosphere (LIMS) instrument on Nimbus 7 [*Haggard et al.*, 1986], as well as for the production processing of the UARS L3B data. As applied to UARS data, the algorithm is based on (1), but without the terms related to time. The coefficients in time are updated sequentially for each new data point.

It is not clear why *Khattatov et al.* [1999] go to some length to contend that the UARS L3B data do not produce synoptic maps. Although the statement is accurate, these data were not meant nor claimed to be synoptic representations, as their generation does not incorporate a physical model. In the documentation for the L3B data [*Huang and Reber*, 1993], it is stated that "the sequential estimation algorithm used to generate the coefficients is based on the stationary form of the Kalman filter. The stationary form is chosen due to insufficient knowledge of an equation of state, necessitating the update of the covariance matrix in an ad hoc manner" (p. 2). It is also stated that "To avoid contamination of the output product due to possible local time effects, the data are separated into ascending and descending mode (north-going and south-going) data, and these two sets are treated separately" (p. 2). Further, it is noted that "Problems in interpretation may be caused by the non-synoptic orbital sampling of data in space and time" (p. 6). It appears that the difficulties Khattatov et al. claim with the L3B data are due primarily to a misinterpretation and misunderstanding of the purpose and mathematical construction of the data set. More information can be found at http://grid.gsfc.nasa.gov:8001/ or http://grid.gsfc.nasa.gov:8001/www/l3b_description.html.

The UARS L3B data represent the level 3AL data (level 2 geophysical data evaluated every 4° in latitude) at regular grids in longitude. The algorithm for generating L3B was chosen because it is robust and feasible for production processing. Because of its sequential nature, it is especially useful in cases of data dropouts. For example, with simple averaging, data dropouts of just a few consecutive points in longitude can skew zonal mean values by more than 20%.

Khattatov et al. [1999] also imply that that level 3B should not be used in general because they do not provide synoptic maps. However, because the L3B files separate the data by orbital mode (and therefore by local time), they can be, and have been, used directly in many applications. An example is the work of *Caziani and Holton* [1998], who used the ascending mode L3B, in part to study Kelvin waves. Evaluation of the data at 0° longitude provided the needed information directly.

As noted earlier, we agree with *Khattatov et al.* [1999] that the *Salby* [1982] method and the UARS level 3B data do not provide "synoptic" representations directly. However, we do not agree with them that the only way to overcome this limitation is to supplement observations with prior independent information, such as a physical model. We believe that it is important that "synoptic" approximations can be obtained from measurements alone, as in a mixture of data and model, it can be difficult to trace the effect of each individually. In addition, the physical model must capture all the significant physical processes reflected in the data, and the uncertainties in each must be consistent. Inconsistent processes and uncertainties will likely lead to spurious results. Also, "synoptic" representations from data alone can reveal important properties, properties which may not have been considered in a model. For example, we have noticed significant diurnal variations in CH_4 and N_2O mixing ratios, both of which have chemical lifetimes much longer than 1 day. More details on this are given in section 3.3. In the next section we show how UARS level 3B data can be used as input for generating local time maps of chemically active species and other diurnally varying parameters.

3. Diurnal and Longitudinal Variations Retrieved From UARS Data

This section describes approximations to "synoptic" representations of diurnal variations for mixing ratios, winds, and temperature derived from the UARS L3B data. We present sample maps of ClO and O_3 mixing ratios based on MLS data; of temperature, and $ClONO_2$, NO_2, and CH_4 mixing ratios based on CLAES measurements; and of meridional winds based on HRDI measurements. The L3B data used here are based on version 8 of the CLAES 3AL data, on version 4 of the MLS 3AL data, and on version 10 of the HRDI 3AL data. The data dates are from day 1, 1992, to day 1, 1993 for CLAES and MLS, and day 226, 1992 to day 226, 1993 for HRDI. The HRDI data used do not correspond to year 1992 as there is a data gap between days 154 and 205 of 1992, due to instrument and observatory problems. It is most effective to use data that are of good quality over a period of a year, so we have chosen the interval from day 226, 1992, to day 226, 1993, for this study.

3.1. An Algorithm for Generating "Synoptic" Approximations

The algorithm we use was described by *Huang et al.* [1997], who calculated the diurnal variations of ozone mixing ratios from UARS data and compared them with a chemical model. It has also worked well in representing diurnal variations of UARS temperature and wind measurements [*Huang et al.*, 1994]. The computations take advantage of the nearly complete diurnal coverage over a 36 day cycle, with data available at two local times for each latitude every day.

At a given latitude, longitude, and pressure, the algorithm performs a two-dimensional Fourier least squares estimate, with independent variables of local solar time and day of year, in the form

$$\Psi(t_l, d, z, \theta, \lambda) = \sum_n \sum_m b_{nm}(z, \theta, \lambda)\, e^{i2\pi n t_l}\, e^{i2\pi m d/365} \quad (3)$$

to obtain the set of coefficients

$$\left\{b_{nm}(z, \theta, \lambda)\right\},$$

where

- z altitude (or pressure surface);
- d day of year;
- λ longitude (radians);
- θ colatitude;
- t time (fraction of a day);
- t_l local solar time (fraction of a day);

and

$$t_l = t + \lambda/(2\pi).$$

The indices "n" and "m" denote wave numbers in local time and day of year respectively. We use a maximum value for *n* of 2, so diurnal and semidiurnal estimates are calculated. Because it takes ~36 days to sample the range of local times (corresponding to our maximum value for m of 10), we ignore day-of-year variations in the diurnal and semidiurnal coefficients for periods less than seasonal, and do not calculate them for wave numbers larger than 4.

In terms of the variability of the diurnal variations themselves, perhaps the parameter that has been most analyzed is winds. As noted by *Forbes* [1984], there are average tidal structures that cover periods of a month or more, and deviations from the average of a few days to a month. *Vial* [1989] notes that monthly averages are more appropriate in the climatological sense. We cannot model the shorter-term deviations of a few days because of the 36 day period required to sample the range of local times. Although the smaller, shorter-term variations will be smoothed out, our analysis contains enough information (coefficients) to reflect the larger variability of tidal structures from day to day. For diurnal variations of temperature, *Wu et al.* [1998] treat the shorter-term variations similarly based on UARS MLS data. Their method is different from that used here in that they take day-night differences and subtract the mean on a daily basis. They also use a 100-day moving window "to reduce remaining systematic noise as much as possible but retain seasonal and longer-term tidal variability" [*Wu et al.*, 1998, p. 8911]. This window is supported by their comparison with the Canadian Middle Atmosphere Model. For constituents, there seem to be fewer documented studies. An indication of the shorter-term fluctuations of $ClONO_2$ and our "goodness of fit" can be seen in Figure 4. We defer discussions of this until section 3.2.

The algorithm minimizes the sum of the squares of the differences between the Fourier series (equation (3)) and the L3B data over a 1 year period. In least squares estimation, when there are two independent variables and the data are not at regular intervals, the conventional method is to first

perform averaging (binning) or interpolation to regular grids. The estimate is then made sequentially, one dimension at a time. This is not feasible for UARS since there are data values at only two local times for each day. We do not average or bin the data, but minimize the square of the differences between (3) and the data for all data in the same step. We are not aware of previous implementations like this, except for that of *Huang et al.* [1997]. As noted below, we have performed extensive tests, showing that this method works well.

The data provide values for a given day at the standard UARS latitudes and pressure surfaces [Computer Sciences Corporation, 1991] and selected longitudes. As background, we note some of the properties of Fourier series least squares estimation: (1) It does not require sampling at regular intervals of the independent variables (day of year and local solar time). (2) It is relatively tolerant of data gaps (several days, at least). Inordinately large data gaps, however, can create difficulties and limit the viable order of the Fourier series expansion, especially when the data contain significant noise or uncertainties. (3) The algorithm (like all implementations of finite, discrete, Fourier series) is susceptible to the problems of aliasing and leakage. These problems can be caused by undersampling, the finite length of the data, the existence of frequencies in the data not at the Fourier frequencies, or lack of periodicity in the data. (4) Under certain conditions, least squares estimates can retrieve coefficients accurately even when the data are sampled at irregular intervals (in which case the covariance matrix is not diagonal). When the matrix is not diagonal and there are nonnegligible higher-order terms, the values of the coefficients can depend on the number of coefficients estimated, thus causing additional aliasing [e.g., *Carnahan et al.*, 1969].

We have performed tests that show the algorithm can accurately retrieve results from inputs consisting of linear combinations of sines and cosines at the Fourier frequencies. The test input was based on sampling patterns in local time and day of year of the MLS measurement track for 1992. Tests show that the off-diagonal elements of the covariance matrix are relatively small, and hence the matrix inversion needed to obtain the coefficients is quite stable, so "additional aliasing" is not a problem. In sections 3.5 and 3.6 we also compare the estimated diurnal components for winds and temperature with the theoretical model of *Forbes and Gillette* [1982], where the good agreement lends further confidence that the different components (diurnal and semidiurnal) are mostly uncorrelated. Therefore, irregular sampling and data dropouts do not appear to be a serious problem in this application. The UARS sampling over local times (every 20 min) is such that higher harmonics than semidiurnal could be retrieved, although we have not done so.

Tests have also shown that the algorithm can properly separate variations with local time from those in day of year. Details are given by *Huang et al.* [1997] for applications to ozone mixing ratios, who make comparisons to a photochemical model.

No attempt has been made to remove year-to-year trends. The data are approximately cyclic over a 1 year period, so trends and leakage are not significant problems. A current limitation of the technique is that results can be obtained reliably only at latitudes within 32° of the equator. This is because poleward of 32°, data are missing on alternate yaw months (~36 days), and that gap is too large to allow confidence in the results.

Our estimates here focus on diurnal variations, as a function of local solar time and day of year. Variations with longitude are reflected through the local time and the coefficients $\{b_{nm}(z,\theta,\lambda)\}$ in (3). Because it takes a half day to sample the range of longitudes using both orbital modes, phenomena with periods less than a few days (e.g., 2 day traveling waves in longitude) that are not coupled to local solar time could show some deviation from the synoptic case in our maps. It is possible to generate mathematical representations of the longitude variations for the coefficients $\{b_{nm}(z,\theta,\lambda)\}$ as well, but this is not expected to effect our results significantly and is beyond the scope of this study.

3.2. Results for ClO, $ClONO_2$, and NO_2

The constituents ClO, $ClONO_2$, and NO_2 are presented together because their diurnal variations are pronounced, and are in large part due to their chemical interactions. *Dessler et al.* [1996] have investigated the partitioning between ClO and $ClONO_2$ using UARS data by analyzing day-night differences of averages over a range of latitudes and a time period of several months. They point out that the sum of the mixing ratios of ClO and ClONO2 in an air parcel is nearly constant over days to weeks. To a good approximation, (R1) and (R2) below, from Dessler et al., are the main reactions related to our results at 10 hPa. During the day, $ClONO_2$ is destroyed by photolysis. Although there are intermediate reactions, they are relatively fast, and effectively we have

$$\text{(R1)} \qquad ClONO_2 + h\nu \longrightarrow ClO + NO_2.$$

$ClONO_2$ is recovered by recombination through the reaction

$$\text{(R2)} \qquad ClO + NO_2 \xrightarrow{M} ClONO_2.$$

As pointed out by Dessler et al., during most of the daylight hours the production and loss of $ClONO_2$ is in steady state. As the Sun sets, the photolysis of $ClONO_2$ decreases while the recombination of ClO and NO_2 continues. The transition period is on the order of one hour, after which ClO is depleted.

Figure 1a shows a latitude-local time map at 10 hPa, for day 75, 1992, of $ClONO_2$ mixing ratios based on zonal means of the data, making it relatively straightforward to compare with chemical models for equinox. Figure 1b shows a similar map for ClO. There is a bias in the ClO data [*Waters et al.*, 1996] such that nighttime values are sometimes negative. Estimates south of -20° latitude are not shown because of isolated anomalous values in the MLS data. Overlooking the bias in ClO, note that the qualitative relationship between the ClO and $ClONO_2$ mixing ratios is quite consistent with the behavior discussed by *Dessler et al.* [1996]. Figure 1c is a map of results for NO_2 corresponding to Figures 1a and 1b. In all cases, the zonal means are taken from the first coefficient of the appropriate level 3B data. Figure 2a shows results for $ClONO_2$ mixing ratios on latitude-longitude coordinates for day 75, 1992, at 10 hPa and 0000 GMT. Figure 2b is a map of ClO, while Figure 2c shows NO_2. Figures 2a-2c represent the approximation to the "synoptic" local time-longitudinal behavior. By comparing these figures to those showing local time variations alone, one can get a qualitative feel for variations induced by longitudinal effects.

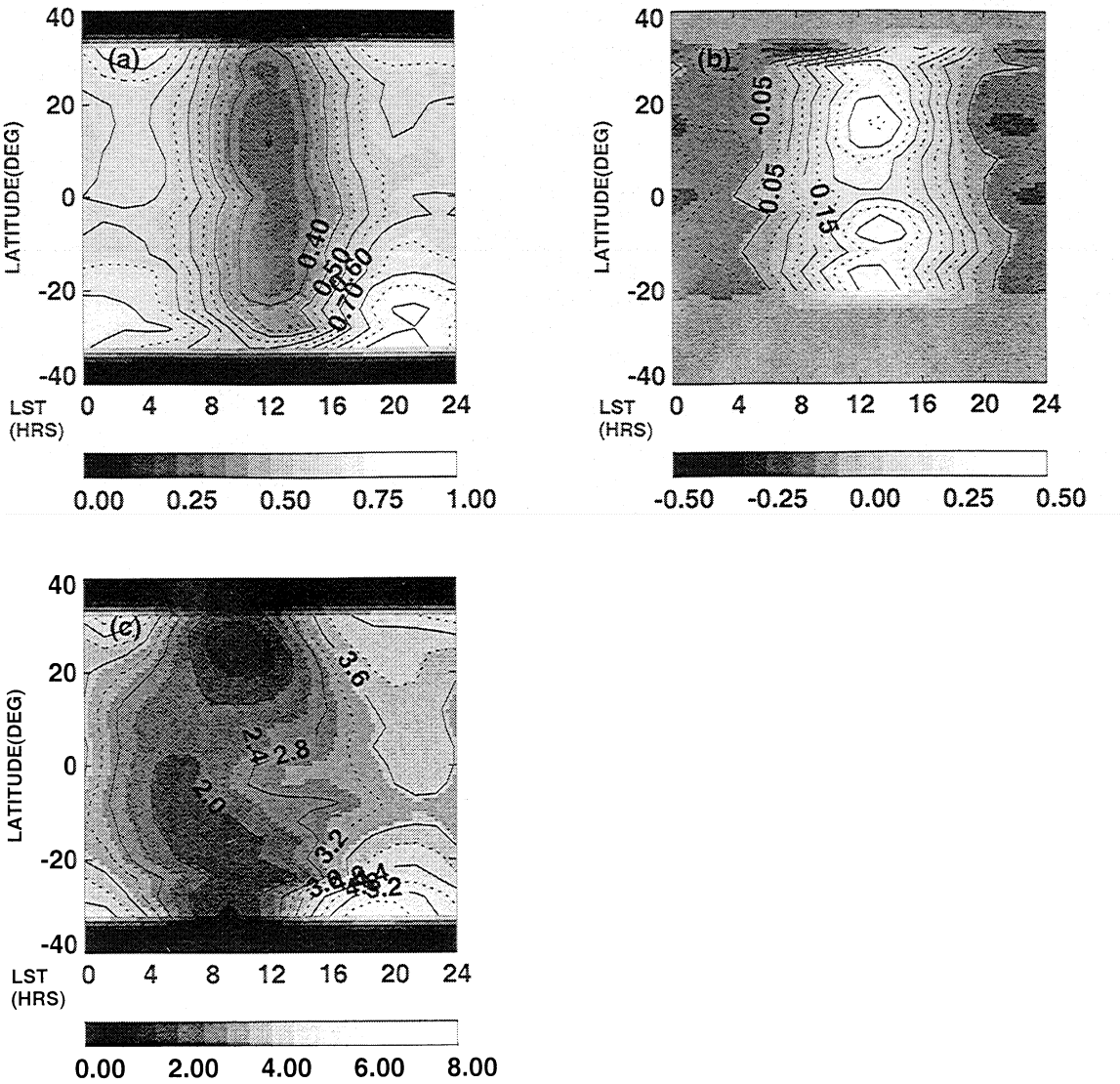

Figure 1. (a) Latitude-local solar time map of CLAES $ClONO_2$ mixing ratios (ppbv) for day 75, 1992, at 10 hPa, based on data zonal means. (b) As in Figure 1a, also based on zonal means, but for MLS ClO (ppbv). There is a bias in the ClO data, so that the nighttime values are sometimes negative. Values south of -20° latitude are not shown because of isolated anomalous values in the MLS data. (c) As in Figure 1a, but for CLAES NO_2 (ppbv) zonal mean mixing ratios. LST, local solar time.

Using averages over latitude for a period of several months, and adjusting for the bias in ClO, *Dessler et al.* [1996] have concluded that the UARS data are consistent with theory. Using our mathematical representations, it is feasible to go a step further and generate diurnal results for any time of year. Because of the relatively high scatter, uncertainties, and biases in the ClO data, it would be worthwhile to wait for the upcoming version of MLS data for ClO, which is due shortly.

The next two figures give an indication of how the estimates relate to the measurements. Figure 3 is a plot of ascending mode $ClONO_2$ data on day 75, 1992, as a function of longitude, showing explicitly the variation in local solar time as a function of latitude. As noted in section 2.1, although the local times of the data are different for various latitudes, they are essentially constant (within 20 min per day) for a given latitude. Consequently, the variations with local time seen in Figure 2a are not present in Figure 3.

Figures 4a and 4b are results based on $ClONO_2$ mixing ratios as a function of local time at 10.0 hPa and 0° longitude, and 0° latitude and 28°N latitude, respectively. The diamonds denote the data, which are taken over the yaw period from day 45 to day 85, 1992. The plusses represent the values when the Fourier series is evaluated on the same day and local time as the measurements. The curves represent the estimates for a single day, namely day 75, 1992. As expected, the Fourier estimates of the diurnal variation match the data better when they are evaluated on the same day and at the same local time as the data, than when they are evaluated for only day 75. The differences between the estimate for day 75 and the data are due to day-of-year variations in the data between days 45 and 85. The difference between the estimate and the data is larger at 28°N latitude than at the equator because the daily variations in the data are more pronounced at 28° latitude; the algorithm has partitioned variations with respect to local time versus variations with day of year accordingly. As can be seen

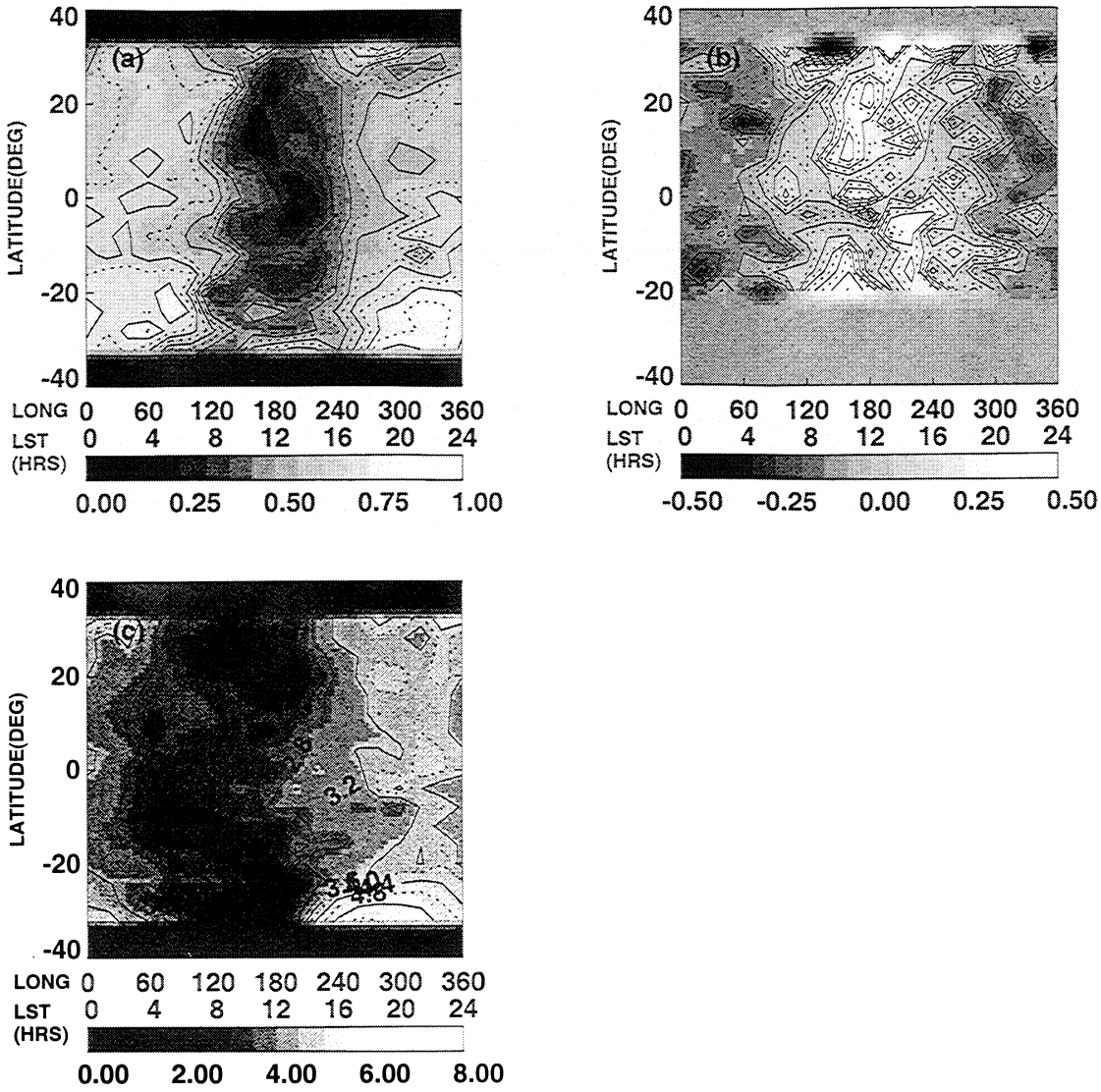

Figure 2. (a) As in Figure 1a, but on a latitude-longitude grid, based on CLAES $ClONO_2$ data at various longitudes (instead of zonal means), at 0000 GMT. (b) As in Figure 1b, for MLS ClO (ppbv) mixing ratios, but based on data at various longitudes, at 0000 GMT. (c) As in Figure 1c for CLAES NO_2, but based on data at various longitudes, at 0000 GMT.

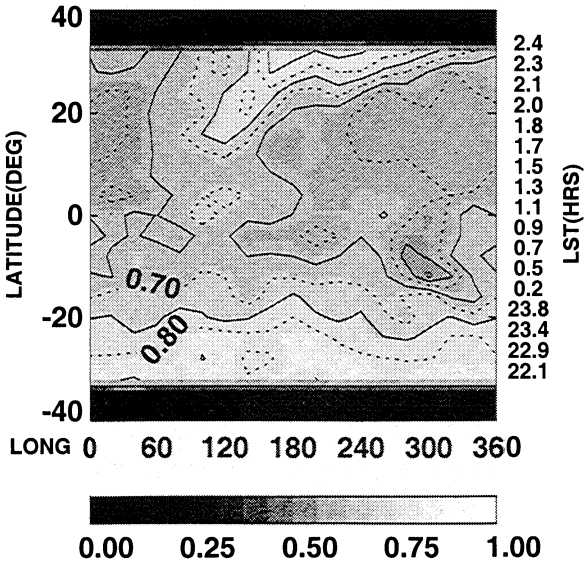

Figure 3. As in Figure 2a for $ClONO_2$, but with the local solar times taken from the level 3B ascending mode data (labeled on right axis). As explained in the text, the local times of the data are different for various latitudes, but are essentially constant (within 20 min) for a given latitude. Consequently, the variations with local time are not present here in comparison with Figure 2a.

in Figure 4, there are higher-frequency phenomena in the data with periods of several days that are not reflected in our Fourier series estimate. For the 10 harmonics we calculate, the shortest period in day of year of the Fourier series is 36.5 days.

3.3. Results for CH_4 and N_2O

Figure 5a is a map of CH_4 mixing ratios based on zonal mean data, for day 75, 1992 at 0.46 hPa, on a latitude-local time grid. Unlike NO_2, $ClONO_2$, and ClO, CH_4 has a chemical

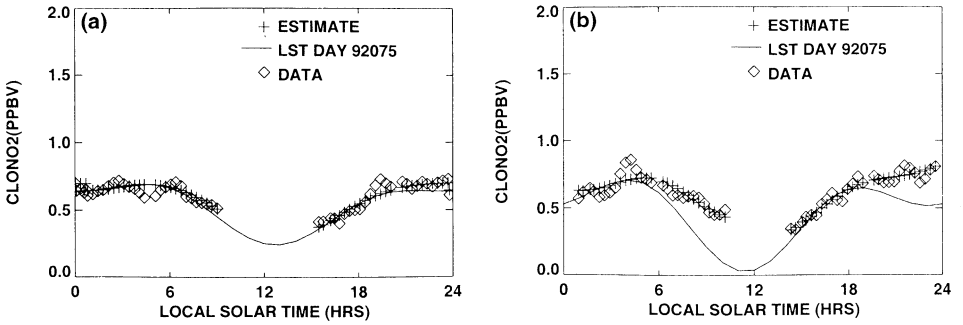

Figure 4. (a) CLAES $ClONO_2$ mixing ratios (ppbv) as a function of local time at 10.0 hPa, 0° latitude, 0° longitude and (b) 28°N latitude, 0° longitude, for day 75, 1992. The diamonds denote the data, which are taken over the yaw period from day 45, 1992, to day 85, 1992 (recall that data are available at only two local times for any given day, and it takes ~36 days to sample the range of local times). The plusses denote the values when the Fourier series is evaluated at both the same day and local time of the data. The curves represent the estimates for 1 day, namely day 75, 1992, as a function of local time. As expected, the Fourier estimates (plusses) match the data (diamonds) better when they are evaluated at both the same day and local time of the data, compared to representing the diurnal variation only for day 75 (lines). For Figures 4a and 4b, the larger differences between the line and the data are because there are also variations with respect to day of year between days 45 and 85 in the data. In addition, the differences between the line and the data are larger in Figure 4b compared to Figure 4a. This is because the variations with respect to day of year in the data (diamonds) are more pronounced at 28° latitude, and the algorithm has partitioned variations with respect to local time versus variations with day of year accordingly.

lifetime much longer than 1 day. However, our study shows that the variation of CH_4 contains significant diurnal variations, occasionally approaching 30%; a preliminary analysis indicates that this is consistent with transport by thermal tides. We are not aware of previous results of this kind for CH_4. Although not shown, the situation is similar for N_2O mixing ratios. Figure 5b, which corresponds to Figure 5a, but on a latitude-longitude grid, represents the approximation to the "synoptic" local time-longitudinal behavior.

Figure 6a shows CLAES CH_4 zonal means at the equator for 0.46 hPa as a function of day for the yaw period covering days 45-85, 1992. The asterisks and curve denote ascending and descending orbital mode data, respectively. As noted in section 2.1, for each mode, latitude, and day, the local time at which the data are sampled is essentially constant, over all longitudes. Because they are zonal means, the differences between the two curves in Figure 6a are attributed to variations with local time. In Figure 6b the diamonds are the same data plotted as a function of local time. The plusses are our estimates evaluated at the same days and local times as the data.

In addition, although there is still a significant amount of work to be done, we have made order-of-magnitude estimates

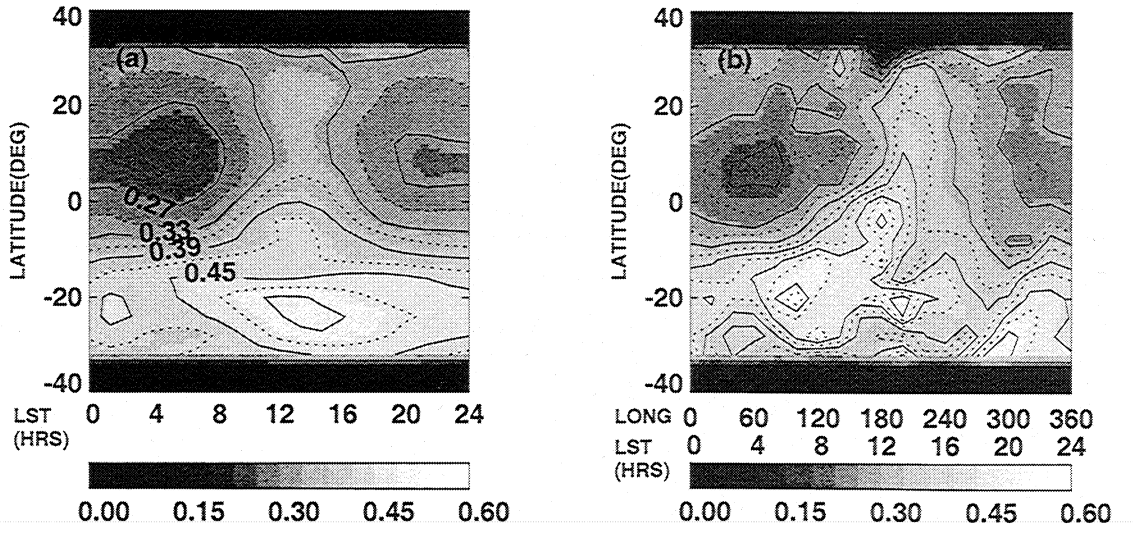

Figure 5. (a) Latitude-local time map of CLAES CH_4 mixing ratios (ppmv), based on zonal means, for day 75, 1992, at 0.46 hPa. Although CH_4 has a chemical lifetime much longer than 1 day, our analysis shows that CH_4 also exhibits significant diurnal variations (at times approaching 30% or more, but usually less, depending on the circumstances). (b) As in Figure 5a, but on a latitude-longitude coordinate, for estimates based on data at various longitudes (instead of zonal means), at 0000 GMT.

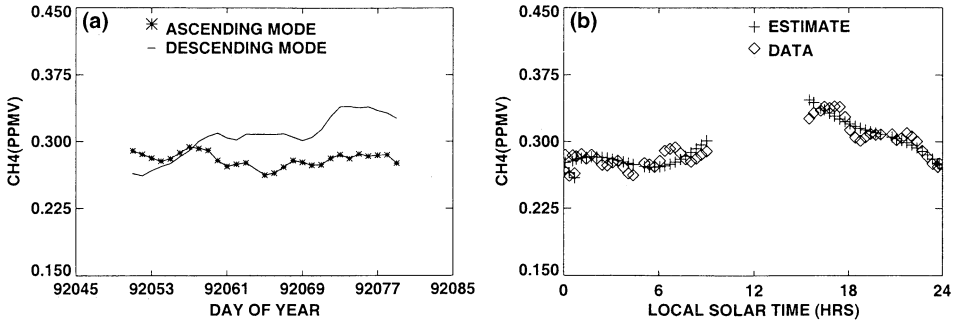

Figure 6. (a) CLAES CH_4 mixing ratio zonal means versus day for the yaw period from day 45, 1992 to day 85, 1992 at the equator and 0.46 hPa, for ascending and descending orbital modes. As noted in the text, the local times of the data for each orbital mode are essentially constant for a given latitude and day, irrespective of the longitude. Therefore the data are sampled at basically two local times each day. Because they are zonal means, the differences in the mixing ratios between the two modes for a given day are attributed to variations with local solar time (LST). (b) As in Figure 6a, but plotted versus local time. The diamonds denote the data, and the plusses denote our estimates evaluated at the local time and day of the data. The local time corresponding to the ascending mode data is 0901 LST for day 51, 1992, and decreases by ~20 min per day, so that it is 0248 LST on day 70, 1992, and 2348 LST on day 79, 1992. For the descending mode, the local time is 0006 LST on day 51, 1992, 1824 LST on day 70, and 1530 LST on day 79.

of the vertical transport velocity by using the equation of continuity. The results indicate that the values of these velocities are in the range of cm/s and are in the neighborhood of theoretical expectations [*Forbes and Gillette*, 1982].

3.4. Results for O_3

Between 10 and 0.46 hPa, at low latitudes, the diurnal variations of O_3 range from a few percent at lower altitudes to ~25% near 0.46 hPa. Figure 7a is a map of O_3 mixing ratios based on MLS zonal mean data from the 205 GHz channel, at 10 hPa, for day 75, 1992, on a latitude-local time coordinate system. Figure 7b corresponds to Figure 7a, but at a pressure of 2.15 hPa, and Figure 7c is a corresponding plot at 0.46 hPa. As can be seen from Figure 7a, the diurnal variations of O_3 mixing ratios at 10 hPa tend to be small on a percentage basis. In Figure 7b the diurnal variations at 2.15 hPa appear to be more prominent, and the mixing ratios tend to maximize shortly after noon. In Figure 7c the mixing ratios at 0.46 hPa appear to minimize around noon, with lowest values near 20° north and south. This behavior is a good test for both the data analysis and photochemical models, and has been presented by *Huang et al.* [1997]. There, using the same algorithm as here, estimates of diurnal variations in the data compared very well with those from a photochemical model at 28° latitude near equinox. The model demonstrated that the changes in the times and altitudes of O_3 minima and maxima at 2.15 and 0.46 hPa are due primarily to oxygen photochemistry. At 10 hPa the model results showed that photochemical effects are not significant, and differences between the model and data results are relatively large. This could be explained by the lack of dynamics in the model. Comparisons at other latitudes and days have not yet been made. Again, Figure 7d, the estimate for O_3 at 2.15 hPa on a latitude-longitude grid, represents the approximation to the "synoptic" local time-longitudinal behavior corresponding to Figure 7b.

3.5. Results for Winds

In this section, we show our estimates based on HRDI measurements of meridional (northward) winds at 95 km (the only altitude at which HRDI measures at both day and night). HRDI-based results on Sun-driven migrating tides are well known [*Hays et al.*, 1992; *Morton et al.*, 1993; *Burrage et al.*, 1996; *Khattatov et al.*, 1997]. The first three are primarily comparisons of zonal averages with the symmetric (1,1) mode, while Khattatov et al. used a numerical model in conjunction with the data to estimate diurnal components over a range of altitudes. Figure 8a is a latitude-longitude plot of our results showing migrating tides in the meridional winds (m/s) at 95 km for day 84, 1993, based on zonal means of the data. Day 84, 1993 was chosen to represent equinoctial conditions (instead of equinox 1992 for the other data) because there is a 50 day gap in the HRDI data beginning with day 154, 1992. Figure 8b presents the results as in Figure 8a, but includes nonmigrating tides as well, based on L3B data evaluated at 20° intervals in longitude. A comparison of Figures 8a and 8b shows distinct differences, with the nonmigrating tides displaying additional variations. Figures 8c and 8d correspond to Figures 8a and 8b respectively, but for solstice conditions (day 355, 1992). *Hagan et al.* [1997] present theoretical estimates which include nonmigrating tides by considering differential heating in longitude due to absorption of solar energy by water vapor and latent heat release associated with cloudiness and rainfall. Their results include the diurnal components of the nonmigrating tides at 99 km, up to zonal wave number 5. A qualitative comparison between results from Hagan et al. (for April, not shown here) and Figure 8b shows that there is more longitudinal structure in our estimates. This may be because our results include both diurnal and semidiurnal components, while Hagan et al. show only diurnal components. There also appear to be systematic phase shifts between Hagan et al.'s calculations and our results based on HRDI data. The 3 km difference in altitude could account for these differences. In addition, the differences between our results for equinox and solstice are more pronounced than those of Hagan et al.

Figures 9a and 9b show the diurnal amplitudes (m/s) and phases (hour of maximum value) at 95 km as a function of latitude for day 84, 1993, corresponding to Figure 8a. The

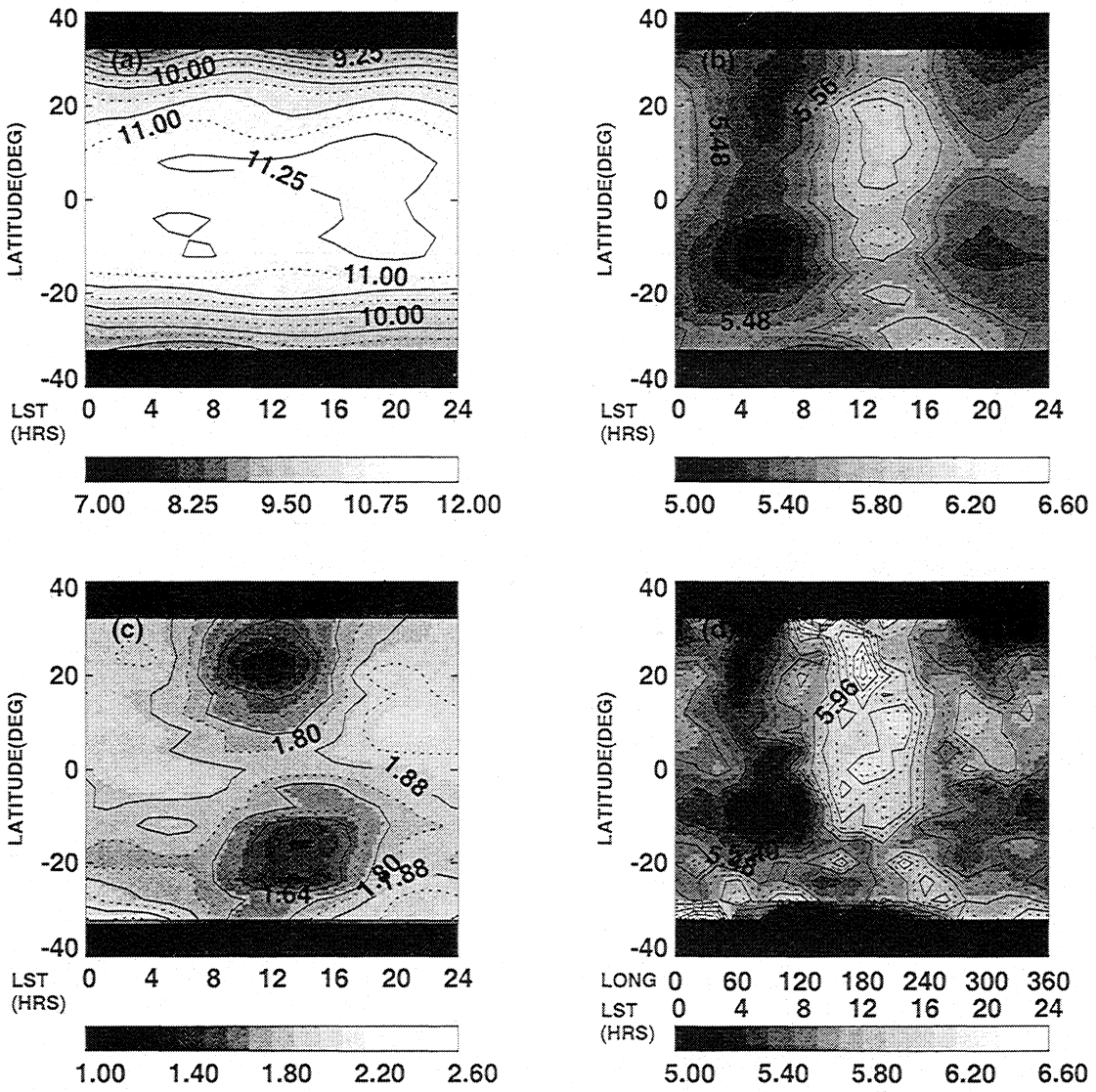

Figure 7. (a) Latitude-local time map based on MLS O_3 (205 GHz channel) mixing ratio (ppmv) zonal means, at 10 hPa, for day 75, 1992. (b) As in Figure 7a, zonal means, but at 2.15 hPa. (c) As in Figure 7a, zonal means, but at 0.46 hPa. Compared to Figure 7b, where the O_3 mixing ratios at 2.15 hPa tend to maximize shortly after noon, the mixing ratios at 0.46 hPa tend to be a minimum around noon. The altitude transition region depends on latitude. At 28° latitude, the results agree very well with the chemical model described by *Huang et al.* [1997]; comparisons at other latitudes have yet to be done. (d) As in Figure 7b, but based on data at various longitudes instead of zonal means, on a latitude-longitude grid.

phases are plotted redundantly to avoid discontinuities. The asterisks denote our results based on HRDI data, and the triangles are from the theoretical model of *Forbes and Gillette* [1982], at 96.6 km, for migrating tides. The expected change of phase of ~12 hours near the equator helps to verify the results. Figures 10a and 10b show the semidiurnal amplitudes (m/s) and phases (hour of maximum value), respectively, at 95 km as a function of latitude for day 84, 1993, corresponding to Figure 9.

3.6. Results for Temperature

To further demonstrate the sensitivity of the algorithm, we include temperature, as its diurnal variations in the stratosphere are relatively small (a few percent). Figures 11a and 11b are plots of diurnal amplitude (K) and phases based on zonal means of CLAES temperature measurements, for day 75, 1992, at 0.46 hPa, as a function of latitude, along with the model predictions of *Forbes and Gillette* [1982] at 52.7 km. It can be seen that the agreement with the model is generally good. As in the case of winds, the agreement between our estimates and those of *Forbes and Gillette* is poorer at solstice, where their results show relatively little change with season. The seasonal variations in our results are more consistent with the results of *Wu et al.* [1998], based on MLS temperatures.

4. Discussion and Conclusions

We have reviewed some of the differing views on, and methods for the generation of, "synoptic" representations from asynoptic satellite data. These include the method by

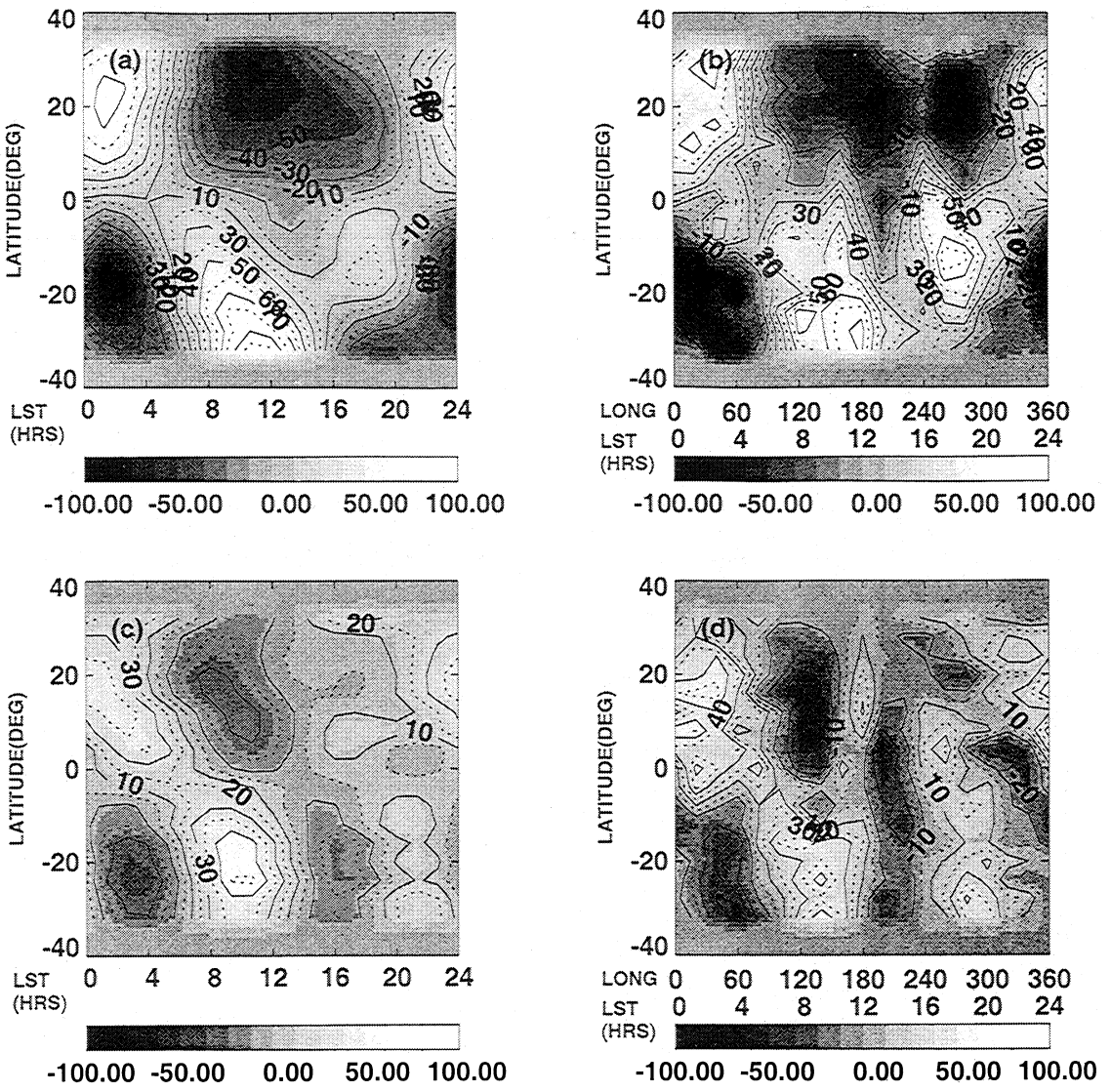

Figure 8. (a) Latitude-local time plot of meridional winds (m/s) at 95 km for day 84, 1993, based on zonal mean HRDI data, more appropriate to migrating tides. (b) As in Figure 8a, but based on data at various longitudes, on a latitude-longitude grid. A comparison of Figures 8a and 8b shows distinct differences, with the nonmigrating tides displaying additional variations. (c) As in Figure 8a, but for day 355, 1992. (d) As in Figure 8b, but for day 355, 1992.

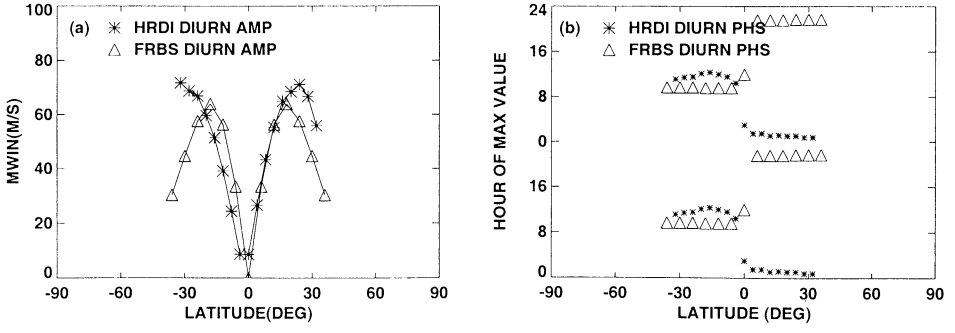

Figure 9. (a) Diurnal amplitudes (m/s) based on zonal mean HRDI meridional winds at 95 km as a function of latitude for day 84, 1993. The asterisks denote results based on HRDI data, and the triangles are from the theoretical model of *Forbes and Gillette* [1982], at 96.6 km, for migrating tides. (b) As in Figure 9a, but for diurnal phases (hour of maximum value) at 95 km as a function of latitude for day 84, 1993. The phases are plotted redundantly to avoid discontinuities.

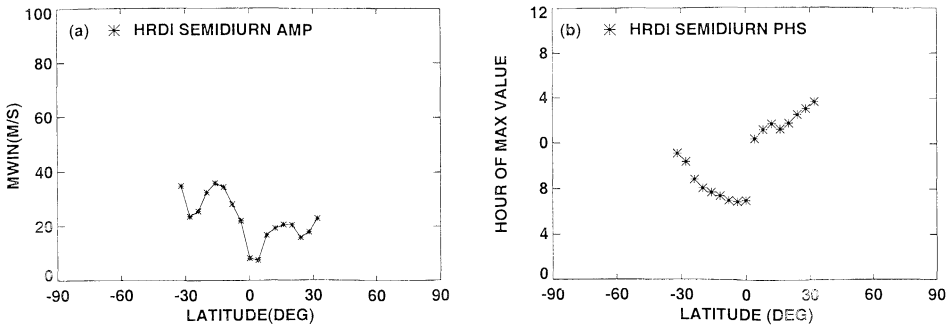

Figure 10. (a) As in Figure 9a, but for semidiurnal amplitudes (m/s). (b) As in Figure 9b, but for semidiurnal phases (hour of maximum value).

Salby [1982] and the sequential estimation technique used to generate UARS level 3B data. In agreement with *Khattatov et al.* [1999], we do not believe that these methods produce synoptic maps of UARS data. As noted in section 2.3, the L3B data were not intended nor claimed to be "synoptic." However, we disagree with the inference by *Khattatov et al.* that since they are not "synoptic", the UARS L3B data should not be used. These data, used and interpreted appropriately, provide a very useful data set for many applications and studies. We have shown how these data can be used as input for an approximation to "synoptic" maps that includes both longitude and local time.

We do not agree with *Khattatov et al.* [1999] that the only way to produce useful "synoptic" approximations is by assimilation with physical models. We have produced "synoptic" approximations for ClO, $ClONO_2$, NO_2, CH_4, O_3, winds, and temperature, based on UARS data alone, without the benefit of physical models. Mixing ratios of ClO, $ClONO_2$, NO_2, and meridional winds exhibit relatively strong diurnal variations, while the magnitude of the variations for O_3, CH_4, and temperature is less. We have compared our estimates for winds and temperature with the theoretical results by *Forbes and Gillette* [1982], and they are encouraging. For winds, our estimates include nonmigrating tides and semidiurnal components as well as diurnal components, and these do not appear to have been demonstrated previously. Although not shown here, in a previous work we compared corresponding results based on MLS ozone data with a photochemical model [Huang et al., 1997] at 28° latitude and equinox. There, the model and data results were compared at more pressure surfaces than the maps shown in section 3.4, and were based on percentage deviations from midnight values. The model and the data agreed well in the change in regime from a maximum in the afternoon at 3 hPa, to an intermediate state at 2.15 and 1.47 hPa with reduced diurnal variation, to the regime at 1 hPa and above with a minimum in the afternoon. We have shown here that CH_4 also exhibits diurnal variations, although its chemical lifetime is much longer than 1 day. In this case also, we are not aware of previous work with comparable results.

An additional advantage of this technique is that the Fourier series containing diurnal variations can be evaluated for different days or times of the year, permitting study of possible systematic changes in this important parameter. Similarly, the form of this representation allows diurnal variations to be extracted separately from other variations, so that variations due to chemistry or dynamics can more easily be identified.

Although our estimates are relatively good "synoptic" approximations, it should be noted that they do not necessarily reflect all the processes measured by the relevant instruments. An indication of how well the algorithm reflects the data was given in Figure 4 for $ClONO_2$. We have quantified diurnal and semidiurnal variations for winds and have presented maps that also include explicit variations with longitude. While data assimilation is important, especially for prediction, it is also important that "synoptic" approximations based on data alone be made available. Otherwise, it is

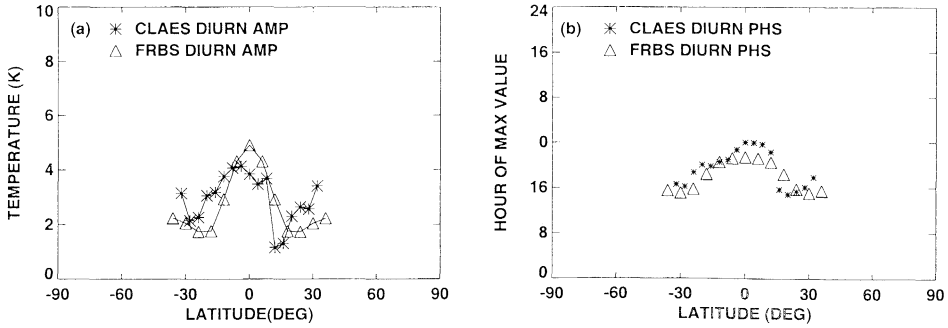

Figure 11. (a) Plot of diurnal amplitudes (K) based on the zonal means of CLAES temperature measurements, for day 75, 1992, at 0.46 hPa, as a function of latitude. Asterisks denote results based on the data, and diamonds denote results from *Forbes and Gillette* [1982] at 52.7 km. (b) As in Figure 11a, but for diurnal phases (hour of maximum value).

difficult to determine which effects are due to data and which are due to the physical model. Further, the measurements and the model should contain the same physical processes. For example, we have seen that the UARS measurements of CH_4 (and N_2O) exhibit diurnal variations (by as much as 30%) even though their chemical lifetimes are much longer than a day. We believe that these diurnal variations are due to transport by thermal tides (work in progress). If such processes are not in the physical model, inconsistencies will manifest themselves. In addition, physical models and their errors must be consistent with the data. Otherwise, the relative weighting of each in the assimilation process could improperly overemphasize one or the other.

Acknowledgments. We thank two anonymous referees for their insightful comments.

References

Barath, F. T., et al., The Upper Atmosphere Research Satellite Microwave Limb Sounder, *J. Geophys. Res.*, *98*, 10,751-10,762, 1993.

Burrage, M. D., et al., Validation of mesosphere and lower thermosphere wind from the high-resolution Doppler imager on UARS, *J. Geophys. Res.*, *101*, 10,365-10,392, 1996.

Carnahan, B., H. A. Luther, and J. O. Wilkes, *Applied Numerical Methods*, John Wiley, New York, 1969.

Caziani, P. O., and J. R. Holton, Kelvin waves and the quasi-biennial oscillation: An observational analysis, *J. Geophys. Res.*, *103*, 31,509-31,521, 1998.

Computer Sciences Corporation, UARS CDHF Software System (UCSS) programmer's guide to production software support services, CSC/SD-86/6704/UD4, El Segundo, Calif., July 1991.

Dessler, A. E., S. R. Kawa, A. R. Douglass, D. B. Considine, J. B. Kumer, A. E. Roche, J. L. Mergenthaler, J. W. Waters, J. M. Russell III, and J. C. Gille, A test of the partitioning between ClO and $ClONO_2$ using simultaneous UARS measurements of ClO, NO_2, and $ClONO_2$, *J. Geophys. Res.*, *101*, 12,515-12,521, 1996.

Elson, L. E., and L. Froidevaux, Use of Fourier transforms for asynoptic mapping: Applications to the Upper Atmosphere Research Satellite Microwave Limb Sounder, *J. Geophys. Res.*, *98*, 23,039-23,049, 1993.

Forbes, J. M., and D. F. Gillette, A compendium of theoretical atmospheric tidal structures, *Rep. AFGL TR 82-0173*, Geophys. Dir., Kirtland AFB, N. M., 1982.

Forbes, J. M., Middle atmosphere tides, *J. Atmos. Terr. Phys.*, *46*, 1049-1067, 1984.

Hagan, M. E., J. L. Chang, and S. K. Avery, GSWM estimates of non-migrating tidal effects, *J. Geophys. Res.*, *102*, 16,439-16,452, 1997.

Haggard, K. V., E. E. Remsberg, W. L. Grose, J. M. Russell II, B. T. Marshall, and G. Lingenfelser, Description of data on the Nimbus 7 LIMS map archive tape, *NASA Tech. Pap. 2553*, 1986.

Hays, P. B., et al., Remote sensing of mesospheric winds with the High Resolution Doppler Imager, *Planet. Space Sci.*, *40*, 1599-1606, 1992.

Hays, P. B., V. J. Abreu, M. E. Dobbs, D. A. Gell, H. J. Grassl, and W. B. Skinner, The High Resolution Doppler Imager on the Upper Atmosphere Research Satellite, *J. Geophys. Res.*, *98*, 10,713-10,723, 1993.

Huang, F. T., and C. A. Reber, Upper Atmosphere Research Satellite (UARS), level 3B data description document, version 4.05, UARS Project, Goddard Space Flight Center, Greenbelt, Md., Nov. 18, 1993.

Huang, F. T, C. A. Reber, and P. B. Hays, Retrieval of local solar time information in atmospheric measurements from the Upper Atmosphere Research Satellite, *Eos Trans. AGU*, *75*(16), Spring Meet. Suppl., 84, 1994.

Huang, F. T., C. A. Reber, and J. Austin, Ozone diurnal variations observed by UARS and their model simulation, *J. Geophys. Res.*, *102*, 12,971-12,985, 1997.

Huschke, R. E. (Ed.), *Glossary of Meteorology*, Am. Meteorol. Soc., Boston, Mass., 1970.

Kalman, R. E. A new approach to linear filtering problems, *J. Basic Eng.*, *82D*, 35-45, 1960.

Khattatov, B. V., V. A. Yubin, M. A. Geller, P. B. Hays, and R. A. Vincent, Diurnal migrating tide as seen by the High Resolution Doppler Imager/UARS 1: Monthly mean global meridional winds, *J. Geophys. Res.*, *102*, 4405-4422, 1997.

Khattatov, B. V., J. C. Gille, L. V. Lyjak, G. P. Brasseur, V.L. Dvortsov, A. E. Roche, and J. W. Waters, Assimilation of photochemically active species and a case analysis of UARS data, *J. Geophys. Res.*,*104*, 18,715-18,737, 1999.

Lait, L. R., and J. Stanford, Applications of asynoptic space-time Fourier transform methods to scanning satellite measurements, *J. Atmos. Sci.*, *45*, 3784-3799, 1988.

Morton, Y. T., R. S. Lieberman, P. B. Hays, D. A. Ortland, A.R. Marshall, D. Wu, W. R. Skinner, M. D. Burrage, D. A. Gell, and J. H. Yee, Global mesospheric winds observed by the High Resolution Doppler Imager on board the Upper Atmosphere Research satellite, *Geophys. Res Lett.*, *20*(12), 1263-1266, 1993.

Reber, C. A., The Upper Atmosphere Research Satellite (UARS), *Geophys. Res. Lett.*, *20*(12), 1215-1218, 1993.

Reber, C. A., C. E. Trevathan, R. J. McNeal, and M. R. Luther, The Upper Atmosphere Research Satellite (UARS) Mission, *J. Geophys. Res.*, *98*, 10,643-10,647, 1993.

Roche, A. E., J. B. Kumer, J. L. Mergenthaler, G. A. Ely, W. G. Uplinger, J. F. Potter, T. C. James, and L. W. Sterritt, The Cryogenic Limb Array Etalon Spectrometer (CLAES) on UARS: Experiment description and performance, *J. Geophys. Res.*, *98*, 10,763-10,775, 1993.

Rodgers, C. D., Statistical principles of inversion theory, in *Inversion Methods in Atmospheric Remote Sounding*, edited by A. Deepak, pp. 117-138, Academic, San Diego, Calif., 1976.

Salby, M. L., Sampling theory for asynoptic satellite observations. part I, Space-time spectra, resolution, and aliasing, *J. Atmos. Sci.*, *39*, 2577-2600, 1982.

Sassi, F., and M. Salby, Fast Fourier synoptic mapping of UARS data, *J. Geophys. Res.*, *103*, 10,885-10,898, 1998.

Vial, F., Tides in the middle atmosphere, *J. atmos. terr. Phys.*, *51*, 3-17, 1989.

Waters, J. W., Microwave limb sounding, chap. 8, in *Atmospheric Remote Sensing by Microwave Radiometry*, edited by M. A. Janssen, John Wiley, New York, 1993.

Waters, J. W., et al., Validation of UARS Microwave Limb Sounder ClO measurements, *J. Geophys. Res.*, *101*, 10,091-10,127, 1996.

Wertz, J. R., (Ed.), *Spacecraft Attitude Determination and Control*, D. Reidel, Norwell, Mass., 1986.

Wu, D. L., C. McLandress, W. G. Read, J. W. Waters, and L. Froidevaux, Equatorial diurnal variations observed in UARS Microwave Limb Sounder temperature during 1991-1994 and simulated by the Canadian Middle Atmosphere Model, *J. Geophys. Res.*, *103*, 8909-8917, 1998.

F. T. Huang, Science Systems and Applications Inc., 5900 Princess Garden Parkway, Suite 300, Lanham, MD 20706. (huang@grid.gsfc.nasa.gov)

C. A. Reber, NASA Goddard Space Flight Center, Greenbelt, MD 20771. (reber@skip.gsfc.nasa.gov)

(Received May 16, 2000; revised August 17, 2000;
accepted August 30, 2000.)